

A Simple Method for the Detection of Long-Chain Fatty Acids in an Anaerobic Digestate Using a Quartz Crystal Sensor

Authors:

Takuro Kobayashi, Hidetoshi Kuramochi, Kouji Maeda, Kaiqin Xu

Date Submitted: 2019-03-26

Keywords: inhibition, anaerobic digestion (AD), long-chain fatty acids (LCFA), quartz crystal microbalance (QCM)

Abstract:

In anaerobic digestion (AD), long-chain fatty acids (LCFAs) produced by hydrolysis of lipids, exhibit toxicity against microorganisms when their concentration exceeds several millimolar. An absorption detection system using a quartz crystal microbalance (QCM) was developed to monitor the LCFA concentration during an anaerobic digester's operation treating oily organic waste. The dissociation of the LCFAs considerably improved the sensor response and, moreover, enabled it to specifically detect LCFA from the mixture of LCFA and triglyceride. Under alkaline conditions, the frequency-shift rates of the QCM sensor linearly increased in accordance with palmitic acid concentration in the range of 0-100 mg/L. Frequency changes caused by anaerobic digestate samples were successfully measured after removing suspended solids and adjusting the pH to 10.7. Finally, the QCM measurements for digestate samples demonstrated that frequency-shift rates are highly correlated with LCFA concentrations, which confirmed that the newly developed QCM sensor is helpful for LCFA monitoring in terms of rapidness and usability.

Record Type: Published Article

Submitted To: LAPSE (Living Archive for Process Systems Engineering)

Citation (overall record, always the latest version):

LAPSE:2019.0424

Citation (this specific file, latest version):

LAPSE:2019.0424-1

Citation (this specific file, this version):

LAPSE:2019.0424-1v1

DOI of Published Version: <https://doi.org/10.3390/en10010019>

License: Creative Commons Attribution 4.0 International (CC BY 4.0)

Article

A Simple Method for the Detection of Long-Chain Fatty Acids in an Anaerobic Digestate Using a Quartz Crystal Sensor

Takuro Kobayashi ^{1,*}, Hidetoshi Kuramochi ¹, Kouji Maeda ² and Kaiqin Xu ^{1,3}

¹ Center for Material Cycles and Waste Management Research, National Institute for Environmental Studies, Tsukuba 305-8506, Japan; kuramochi.hidetoshi@nies.go.jp (H.K.); joexu@nies.go.jp (K.X.)

² School of Engineering, University of Hyogo, 2167 Shosha, Himeji 671-2201, Japan; maeda@eng.u-hyogo.ac.jp

³ School of Environmental Science and Engineering, Shanghai Jiao Tong University, Shanghai 200240, China

* Correspondence: kobayashi.takuro@nies.go.jp; Tel.: +81-29-850-2110

Academic Editor: Talal Yusaf

Received: 20 September 2016; Accepted: 15 December 2016; Published: 24 December 2016

Abstract: In anaerobic digestion (AD), long-chain fatty acids (LCFAs) produced by hydrolysis of lipids, exhibit toxicity against microorganisms when their concentration exceeds several millimolar. An absorption detection system using a quartz crystal microbalance (QCM) was developed to monitor the LCFA concentration during an anaerobic digester's operation treating oily organic waste. The dissociation of the LCFAs considerably improved the sensor response and, moreover, enabled it to specifically detect LCFA from the mixture of LCFA and triglyceride. Under alkaline conditions, the frequency-shift rates of the QCM sensor linearly increased in accordance with palmitic acid concentration in the range of 0–100 mg/L. Frequency changes caused by anaerobic digestate samples were successfully measured after removing suspended solids and adjusting the pH to 10.7. Finally, the QCM measurements for digestate samples demonstrated that frequency-shift rates are highly correlated with LCFA concentrations, which confirmed that the newly developed QCM sensor is helpful for LCFA monitoring in terms of rapidness and usability.

Keywords: quartz crystal microbalance (QCM); long-chain fatty acids (LCFA); anaerobic digestion (AD); inhibition

1. Introduction

Waste oil has great potential in renewable energy production because of its high energy density and the large amount generated as a result of human activities. Fat, oil, and grease (FOG) in waste streams produced from restaurant kitchens and food industries is a major problem in the sewer systems of urban areas. FOG deposits formed on pipe walls lead to clogging, which can cause flooding, pollution, and other public health problems. Since direct discharge of FOG into sewer lines is no longer permitted, grease traps are generally installed in commercial facilities to remove FOG before it enters sewer lines. The accumulated oily organic waste, including FOG and food scraps, has a high energy potential. Major forms of energy from those oily organic wastes are biodiesel fuel and biogas. Biogas conversion via anaerobic digestion (AD) technology is a better choice when the waste has a difficult-to-extract oil fraction because of emulsion formation or high water content. The average methane yield from grease trap waste is 767.5 ± 107 mL/g of volatile solids (VS) added, which is higher than those from other kinds of municipal solid wastes (around 500 mL/g-VS added) [1]. Yalcinkya and Malina [2] presented the methane yield from grease trap waste as 845–1050 mL/g-VS added. These very high values are due to the high methane potential of lipids.

Several researchers have demonstrated that the AD of oily organic waste is subjected to inhibition caused by long-chain fatty acids (LCFAs) such as oleic acid, stearic acid, and palmitic acid produced

from hydrolysis of triglycerides, which is one of the main components of FOG. Since β -oxidation is the rate-limiting step in lipid degradation [3], faster hydrolysis of lipids can lead to LCFA accumulation during the AD of wastes with high oil or fat content. Only a few millimolar of concentration of accumulated LCFAs can strongly inhibit methanogens in an anaerobic process [3–6] and result in the failure of operation [7]. The toxicity effect is impacted by temperature and the presence of cations such as calcium and magnesium. Hence the management of LCFA toxicity is considered a promising way to overcome poor performance of a digester due to LCFA accumulation [8]. Roy et al. [9] showed decreased levels of inhibition caused by LCFAs with the addition of calcium ions. On the other hand, Koster [10] demonstrated that only 20 min exposure to 7.5 mmol/L lauric acid, which is the lag time for adding calcium, reduced 67% of the original activity of methanogens. Once inhibited by LCFAs, a digester takes a very long time to recover and produce methane [11]. When treating oily organic wastes, digester operators should timely minimize the inhibitory effect; for example, by adding calcium as soon as the digester shows a trend for LCFA accumulation. For such reasons, routine measurements of LCFAs in a digester are required.

Determination of LCFA concentrations in anaerobic digesters mostly depends on gas chromatography (GC) [1,12–14]. This GC-based method is accurate and reliable but the analytical procedure is complicated and time-consuming. Moreover, GC analysis requires expensive instrumentation. As such, LCFA measurement has not yet been widely adopted in the field of AD; however recent increased interest in the AD of oily waste is likely to create a new need for an alternative method for LCFA analysis that is rapid and easy. Quartz crystal microbalance (QCM) is a widely used sensing device for rapidly detecting target substances in air or water. QCM comprises an AT-cut quartz crystal disc sandwiched between two metal electrodes, which oscillate at a specific frequency when voltage is applied. The frequency is reduced by mass changes on the electrode and allows for monitoring of small mass absorption on the electrode with the use of specific coatings for target substances. Since a strict selective detection targeting only a single compound is in most cases not possible [15], QCM sensors are often applied for versatile detection of substances belonging to specific groups in a total analysis. Although there are no QCM sensing applications for LCFAs and to AD processes, similar compounds, such as volatile fatty acid (VFA) [16] and olive oil [17,18], have been successfully detected using QCM in the gas phase. QCM sensors have mainly been used for detecting trace compounds in air. In recent decades, advances in QCM methodology have enabled liquid applications and some researchers have used QCM measurements to analyze wastewater samples [19,20]. Yang and Zhang [19] showed the selective detection of Cu^{2+} among various metal ions in real wastewater. In addition, our previous studies have demonstrated that QCM can sense the crystallization of lauric acid on the surface of a cooled electrode as a gradual decrease in resonance frequency [21]. These studies indicated that a QCM sensor can quantitatively detect LCFAs in anaerobic digestate. In this study, the performance of a QCM sensor in a selective and quantitative detection of LCFAs is evaluated, and the feasibility for its practical use in monitoring an increasing trend in LCFA accumulation during the operation of an anaerobic digester is investigated. Since the major LCFA species accumulated in digesters treating de-oiled grease trap waste (GTW) is palmitate [7], followed by oleate, palmitate detection is emphasized in the measurements in this study.

2. Materials and Methods

2.1. Materials and Preparation of the Quartz Crystal Microbalance Sensor

A 5 MHz AT-cut quartz crystal with gold electrodes was used in this study. The disc diameter was 25.4 mm. The frequency and series resonance resonance were measured using a frequency counter Model QSR-F-5 (SRC, Itoigawa, Japan). First, the quartz crystal was coated with a polyvinyl butyral (PVB)-based coating reagent (AY-302, Sunhayato, Tokyo, Japan) to reduce the interference caused by the electrolyte in anaerobic digestate, and then coated again with a copolymer of styrene-divinylbenzene (PS-DVB) gel (PLS-2 for AQUA, GL Science, Tokyo, Japan) by random immobilization. PS-DVB was

expected to efficiently absorb LCFAs in the digestate because it showed the highest frequency-shift rate with a lower increase in resonance residence among a total of five materials, including α -cyclodextrin polymer, polyethylene glycol 2000, OV-275, C18-bound PS-DVB gel, and normal PS-DVB gel when they were applied to QCM coating by random immobilization. The PVB-based reagent was diluted eight-fold with ethanol before use. The PS-DVB gel was first disintegrated by bead beading for 5 min, then 20 mg of the gel was dispersed in 10 mL of ethanol. The solution was stirred by a magnetic stirrer.

After rinsing with ethanol, a 15 μ L PVB-ethanol solution including approximately 160 μ g dry weight of PVB was spread on one side of the QCM disc surfaces with a micropipette and dried for approximately 30 min. Then a 3.3 μ L PS-DVB solution, including 6.6 μ g dry weight of PS-DVB obtained from a stirred glass bottle, was spread on the gold electrode with a micropipette. After briefly air-drying, the PS-DVB film was coated twice following the same procedure. In this study, the QCM disc was washed with ethanol to remove the spent coating and was newly coated every time a measurement was carried out to ensure the reproducibility. The flow cell used for the QCM measurements consists of three Teflon pieces (Figure 1). The top piece was the cell top used to hold the reference and counter electrodes, the center piece was the cell body for the solution, and the bottom piece was used for mounting. The quartz crystal was located between the center and bottom pieces, and the seal was formed through two O-rings pressed together by screws. The working volume of the flow chamber created inside the cell was 0.15 mL. The sample was introduced from the inlet port on the top of the flow cell by a peristaltic pump and flowed radially outward from the center of the cell to the exit channel at the edge. The flow rate during the measurement was 0.12 mL/min. All measurements were performed by feeding the sample solution into the flow cell, for approximately 200 s, in at least triplicate for each sample at around 25 °C.

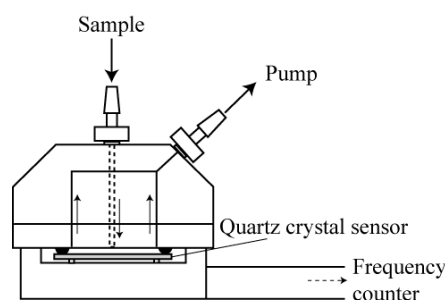


Figure 1. Schematic of the flow cell equipped with quartz crystal sensor. Solid-line arrows indicate travel directions of water.

2.2. Performance of the Quartz Crystal Microbalance Sensor

The QCM response was studied using palmitic acid at different pH ranges (6.0–10.7) and concentrations (0–100 mg/L). Palmitic acid aqueous solution samples were prepared by adding palmitic acid purchased from Wako Pure Chemical Industries (Osaka, Japan) into reverse osmosis-purified water at concentrations of 12.5, 25, 50, and 100 mg/L and the pH was adjusted to specified values by adding 0.1 mol/L HCl or NaOH. Subsequently the solution was heated up to 65 °C in a water bath and stirred by a magnetic stirrer to melt and dissociate the palmitic acid. Finally the pH was adjusted to the specified values at 25 °C, where solid particles of the unionized palmitic acid were present in the aqueous phase at pH 6.0, 7.5, and 9.0; however they were completely dissolved into the water at pH 10.7. To investigate responses of the QCM sensor to several chemicals, triolein (100 mg/L), acetic acid (100 mg/L), and a mixture of palmitic acid (final concentration 100 mg/L) and triolein (final concentration 100 mg/L) samples were prepared similarly. In measurements of anaerobic digestate samples, the QCM system must be operated in a batch mode after pH adjustment and removal of suspended solids. The digestate samples were prepared as follows; 1 mL of digested sludge was first diluted up to 40 times by water and the pH was adjusted to 10.7 by adding 1 mol/L NaOH.

After stirring at 65 °C in a water bath, the pH was adjusted to 10.7 again at 25 °C. Finally, the solution was centrifuged at 5000 rpm for 10 min and the supernatant was used for QCM measurements.

2.3. Reactor Set-Up

The semi-continuous experiment was conducted using a continuously stirred reactor with a working volume of 5 L. The reactor temperature was maintained at 35 °C by hot water circulation in a water jacket. The inoculum was taken from an anaerobic digester of sewage sludge (Shimodate Wastewater Treatment Plant, Ibaraki, Japan) and acclimated to food wastes. The amount of biogas produced from the reactor was measured with a digital gas counter Model μ flow (Bioprocess Control, Lund, Sweden). Hydraulic retention time was gradually shortened from 100 to 25 days by increasing the feeding rate from 50 mL/day to 200 mL/day. The substrate used in this study was de-oiled restaurant GTW. The GTW samples, which typically contain 30–60 wt % oil, were collected from seven restaurants. After each sample, each in a 10 L plastic bottle, was heated up to 60 °C by a hot water bath, the upper oil layers this created were removed [1,7] and the residues (de-oiled GTWs) were mixed together. Thus the lipid content of de-oiled GTW was approximately 54 g/L. The feeding and the withdrawing of sludge were each carried out manually with a glass syringe once a day.

2.4. Validation of Quartz Crystal Microbalance Measurements

Reproducibility of frequency-shift rates was evaluated by seven-cycle measurements of the same digestate sample using a single QCM sensor. The QCM disc was rinsed with ethanol to remove the used coating and coated again in the same manner every time a measurement was carried out. The relative standard deviation (RSD) of the seven values of frequency-shift rates for each sample were calculated from the measurements. The extraction of LCFAs adsorbed onto the sludge was investigated using three sludge samples (A, B and C) taken from the continuously stirred reactor. A 1 mL of digested sludge was diluted up to 40 times by water and the pH was adjusted to 10.7. The pH of the solution was adjusted to 10.7 again at 25 °C after being stirred at 65 °C in a water bath. Subsequently the solution was centrifuged at 5000 rpm for 10 min. The supernatant and sediment were collected to measure LCFAs by GC. All the recovery experiments were performed in triplicate.

2.5. Analysis

The proportions of CH₄, CO₂, and N₂ in the biogas were determined using a gas chromatograph Model GC-8A (Shimadzu, Japan) equipped with a thermal conductivity detector. The stainless-steel column in the gas chromatograph was packed with Shincarbon ST (Shinwa Chemical Industries, Kyoto, Japan). The pH was determined as soon as the sample was collected, using a pH meter Model HM-25R (TOA-DKK, Tokyo, Japan) equipped with a GST-5721C electrode (TOA-DKK, Tokyo, Japan). Total suspended solids (TSS) was determined according to the sewage test methods of Japan Sewage Works Association. Free LCFAs such as caprylic acid (C8:0), capric acid (C10:0), lauric acid (C12:0), tridecanoic acid (C13:0), myristic acid (C14:0), palmitic acid (C16:0), palmitoleic acid (C16:1), stearic acid (C18:0), oleic acid (C18:1), linoleic acid (C18:2), linolenic acid (C18:3), arachidic acid (C20:0), cis-11-eicosenoic acid (C20:1), behenic acid (C22:0), and erucic acid (C22:1) were measured as fatty acid methyl esters using an Agilent 6890 gas chromatograph (Agilent J&W, Santa Clara, CA, USA) with a flame ionization detector. A DB-WAX capillary column (Agilent J&W, Santa Clara, CA, USA) was installed in the gas chromatograph. Fatty acid methyl esters for GC analysis were prepared by the HCl/methanol/toluene method optimized for free fatty acids [22]. First 1 mL digestate samples were lyophilized by a freeze dryer Model DC401 (Yamato, Tokyo, Japan) for at least 6 h to completely remove water from the samples. Then the samples were dissolved in 0.2 mL toluene and mixed with 1.8 mL HCl/methanol reagent in a glass vials. The methylation was performed by heating the mixtures in a metal block for 20 min according to the literature [22] and methyl esters were extracted in the hexane phase after cooling at room temperature and addition of 1 mL hexane and 0.2 mL reverse osmosis-purified water. Acid–base titrations and end point (EP) determination were performed using

an automatic titrator 848 Titrino plus (Metrohm, Herisau, Switzerland) equipped with a pH electrode (Ecotrode Plus, Metrohm, Herisau, Switzerland). The titration was carried out by adding 0.1 mol/L NaOH into the mixed solution of 10 mmol/L LCFAs and HNO₃. The blank solution contained only 10 mmol/L HNO₃.

3. Results and Discussion

3.1. Characteristics of the Quartz Crystal Microbalance Sensor

3.1.1. Effect of Dissociation on Quartz Crystal Microbalance Frequency Responses

Most short-chain fatty acids, such as acetic and propionic acids, have lower pKa values than the neutral pH level, and are easily dissolved in water or digestate in the form of ions; however, the pKa values of fatty acids increase with their carbon chain length. The pKa of C8–C18 chain-length fatty acids has been determined experimentally by titration. The C8, C10, and C12 fatty acids show pKa values below 7.5, and those of C14, C16, and C18 fatty acids are in the range of 8.1–10.15 at 20 °C or 25 °C [23,24]. As described above, palmitate and oleate are predominant LCFAs in an AD of de-oiled GTW [7]. Therefore most LCFAs are almost insoluble in digestate, having a neutral pH. Usually LCFAs are immiscible and float to the water surface like lipids. In contrast, dissociation at alkaline pH allows LCFAs to dissolve into water and, as a result, LCFAs can be successfully dispersed in digestate or water. In this study, to determine the desirable pH for QCM measurements of palmitate, EPs in titrations with NaOH solution were first investigated using palmitic and oleic acids. The titration curves were obtained using palmitic and oleic acids at 25 °C and 65 °C. Palmitic acid has too slow a dissociation rate, making it impossible to obtain a good titration curve using an automatic titrator at 25 °C, while oleate successfully shows an S-shaped curve. The average pH at the EP of oleate is 10.69 ± 0.21 at 25 °C (*n* = 5). By contrast, palmitic acid completely melts at 65 °C and is easily dissociated by the addition of a NaOH solution, and the aqueous solution shows a transparent appearance. The pH finally reaches 10.5 and the palmitate is still dissociated at room temperature. As a result, the average pH values at EPs are 9.32 ± 0.05 (palmitic acid) and 9.48 ± 0.19 (oleic acid). These results are similar to those of Kanicky and Shah [24], suggesting that oleic acid shows a higher pKa than palmitate at 20 °C. On the basis of this nature, the pH values of the samples in this study were adjusted to 10.7 before testing with the QCM sensor.

The QCM response was studied using palmitic acid at different pH levels in the range of 6.0–10.7 to understand the effects of acid dissociation. Figure 2a illustrates typical patterns of frequency shifts at pH values 6.0, 7.5, 9.0, and 10.7 during QCM measurements of 100 mg/L palmitic acid in water. The frequency-shift of the QCM sensor is considered as a mass change of the electrode caused by the absorption of palmitate. The frequency-shift patterns always show linear decreases, except in the initial period. Although in most cases researchers use the values of frequency change after a given period of time, a measurement using a flow cell shows a lag time before sample reach a QCM disc, sometimes resulting in destabilization in sensor response at initial period. Therefore, the absolute values of the slopes of regression lines were calculated using linear portions of frequency curves (basically in the range from 50 s to 150 s) in this study. The bars shown in Figure 2b are the averages of the slopes, indicating decreasing rates in the frequencies. As shown in these figures, the frequency-shift rates are considerably increased in the pH range of 7.5–10.7, crossing the pKa value. The total water-solubility of the palmitic acid including dissociated and nondissociated form (C_{tot}^{sat}) depends on the pH. The C_{tot}^{sat} is determined as follows [25]:

$$C_{tot}^{sat} = \frac{C^{sat}(\text{HA})}{\alpha} = \frac{C^{sat}(\text{HA})}{[\text{HA}]/([\text{HA}] + [\text{A}^-])} = C^{sat}(\text{HA}) \left(1 + \frac{K_a}{[\text{H}^+]} \right) \quad (1)$$

where $C^{sat}(HA)$ is the water-solubility of the nondissociated palmitic acid and $[HA]$, $[A^-]$ and $[H^+]$ are concentrations of the nondissociated palmitic acid, dissociated palmitic acid, and proton, respectively. $C^{sat}(HA)$ is 7.2 mg/L [26] at 20 °C. K_a can be based on the pKa (8.7) of the palmitic acid determined by Kanicky et al. [23] at 20 °C. The total solubility of the palmitic acid (nondissociated and dissociated forms) increases as a function of pH and shows a logarithmic increase up to the solubility product of the palmitate salt under alkaline conditions (pH > 9). Because there is no information about the solubility product of the palmitate salt, the theoretical maximum total solubility is unknown. According to this estimation, although the temperature is a little different, the total solubility values are 22 mg/L at pH 9.0 and 727 mg/L at pH 10.7. This means that 100 mg/L palmitic acid is completely dissolved into water (100 mg/L) at pH 10.7. Interestingly both the total solubility and frequency-shift rate at pH 9.0 were approximately one-fifth of those obtained at pH 10.7. It is clear that the increase in the concentration of the ionized form of palmitic acid, caused by pH elevation, can enhance the response of the QCM sensor. The dissociated forms of fatty acids are water-soluble and have a hydrophobic carbon chain, likely leading to effective absorption onto the PS-DVB film, which has a hydrophobic nature. On the basis of the above facts, we can conclude that pH adjustment as a pretreatment for QCM measurements is a useful strategy.

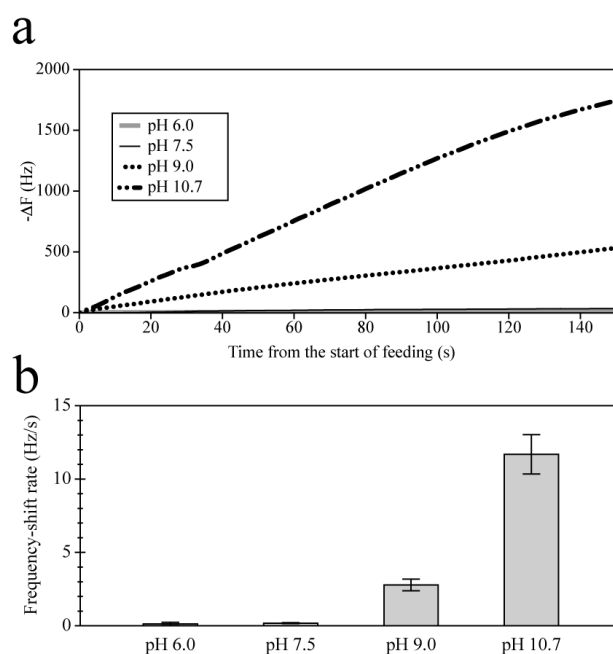


Figure 2. (a) Typical frequency change patterns during quartz crystal microbalance (QCM) measurements of 100 mg/L palmitic acid at different pH levels, the horizontal axis represents the time from the start of feeding into the flow cell; and (b) absolute values of average frequency-shift rates ($n = 3$) within the linear ranges (50–150 s).

3.1.2. Linear Range and Selectivity of the Sensor

Several studies dealing with QCM sensors have presented a very good linear correlation in frequency shift versus concentrations of target substances within a specific range [27–29]. In this study, the linearity in the frequency-shift rate versus solution concentration was evaluated using different concentrations of palmitic acid solutions at pH 10.7. The typical patterns of frequency shift at each palmitate concentration and the average absolute values of frequency-shift rates are given in Figure 3a,b, respectively. All samples of 12.5–100 mg/L palmitate, except the blank solution, similarly show linear decreases for the first 150 s, while their decreasing rates rise according to palmitate concentrations. However, 100 mg/L palmitate shows destabilized frequencies soon after the resonance resistance exceeds 1000 Ω at approximately 160 s. Similarly 150 mg/L palmitate shows a fluctuation in

the frequency curves earlier, around 100 s, when the resonance resistance is over 1000 ohm. Taking this into consideration, the maximum detection limit of our sensor might depend on the oscillator's load capacitance. As such, in this study, 0–100 mg/L is regarded as a reliable range for study. Based on the average frequency-shift rates in Figure 3b, there is a high correlation ($R^2 = 0.9929$) between the rates and palmitate concentrations within 0–100 mg/L. Within the linear range, Sauebery's Equation (2) is established [29].

$$\Delta m = -C \cdot \Delta f \quad (2)$$

In this equation, there is a linear relation between mass change on the electrode (Δm) and frequency shift (Δf). Nevertheless Sauebery's equation is inaccurate when the mass change is greater than 2% of the mass of the quartz disc [30]. In the present study, the mass change due to the coating is $36 \mu\text{g}/\text{cm}^2$ and that estimated from Sauebery's equation, when measuring 100 mg/L palmitate, is at most $15 \mu\text{g}/\text{cm}^2$. Thus the total mass change during our experiment is a level below 0.1% of the quartz disc weight.

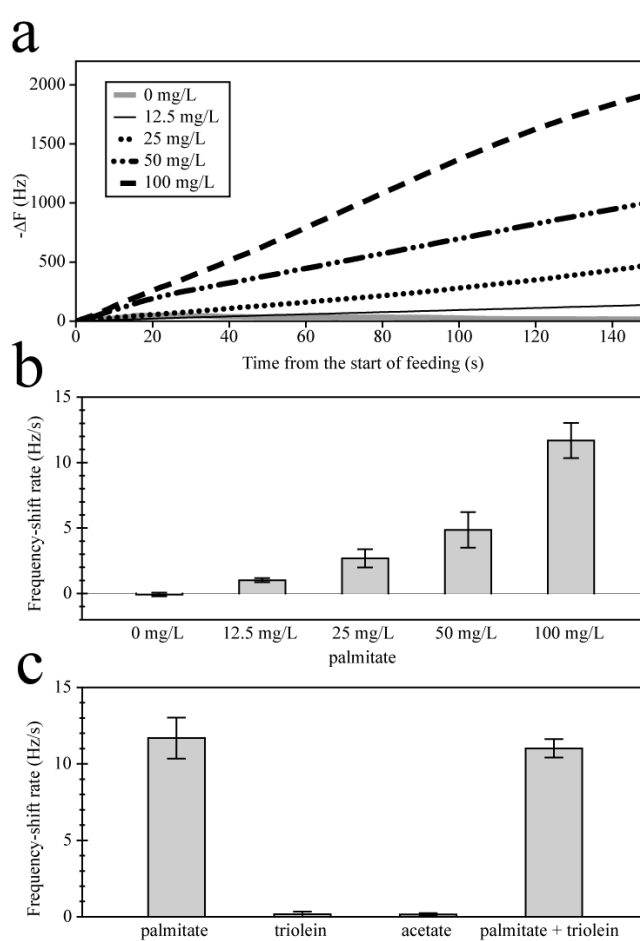


Figure 3. (a) Typical frequency change patterns during QCM measurements using different concentrations of palmitate; (b) absolute values of average frequency-shift rates ($n = 3$) within the linear ranges (50–150 s) at each palmitate concentration; and (c) absolute values of average frequency-shift rates ($n = 3$) within the linear ranges (50–150 s) obtained from solutions of different model compounds.

In AD, due to the relatively high concentrations of LCFAs (50–3000 mg/L) at inhibition levels [3,4,14], such high sensitivity is not required for the QCM sensor. Meanwhile, selectivity is more important because there are various chemicals similar to LCFAs, such as triglycerides and acetate, in the digestate. Figure 3c illustrates the frequency response to various substances based on the average

frequency-shift rates obtained in the same way stated above. All QCM measurements are carried out at pH 10.7. A higher response is clearly observed when the sensor is applied to palmitate-containing solutions. Conversely triolein and acetate show little effect on frequency. In the presence of palmitate and triolein, the QCM sensor shows the same level of response as with palmitate alone. These facts indicate that our QCM sensor can selectively detect palmitate. It is clearly found by observation that triolein is not dissolved and forms a droplet on the surface of the water even at pH 10.7. These droplets of triolein are probably not allowed to flow into the QCM flow cell and thus have no chance to contact the coated film, which is the cause of the low response. It is well known that the water solubility of the hydrophobic compounds with an ionized functional group is generally higher than the solubility of the neutral species and the potential to partition from 1-octanol to water significantly increases by several orders of magnitude. Therefore palmitate in triolein phase can easily transfer to aqueous solution even if palmitate and triolein coexist together. Additionally the low response to acetate is likely due to its hydrophilic nature. These results indicate that pH adjustment and dissociation of fatty acids can contribute to the selectivity of the QCM sensor.

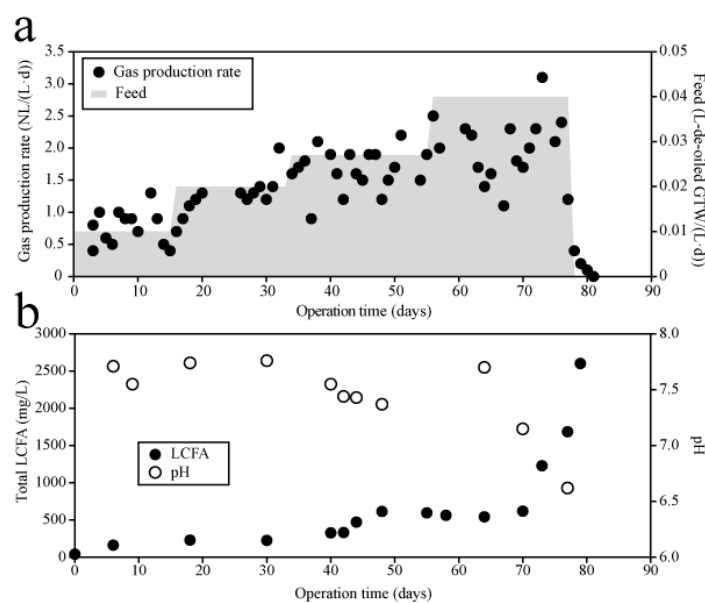
3.2. Feasibility for Practical Use in Anaerobic Digestion Operation

3.2.1. Semi-Continuous Operation of an Anaerobic Digester Treating De-Oiled Grease Trap Waste

A laboratory-scale mesophilic anaerobic digester was operated through gradually increasing the organic loading rate to take digestate samples that include different concentrations of LCFAs. Since the operation performance of the digester treating de-oiled GTW has been detailed in several studies [7,11,31], this study focuses on the evolution of LCFA concentration and methanogenic activity; i.e., the biogas production rate. Figure 4a shows the time courses of gas production rate and feeding rate of de-oiled GTW and Figure 4b shows the shifts of pH and LCFA concentration during the semi-continuous experiment. The main compositions of LCFA species during days 30–79 are summarized in Table 1. The feeding rate is elevated in stages from 0.010 to 0.040 L-de-oiled GTW/(L-reactor·day). The gas production rate gradually increases accordingly during feeding rates of 0.010–0.027 L/(L·day). Methane content in biogas ranges from 56% to 72% throughout this period. After the feeding rate changes to 0.040 L/(L·day), a constant level of gas production rate is maintained for the first 20 days and then the gas production sharply decreases. Finally the gas production is completely inhibited, even when the feeding stops. On the other hand, the pH is within the range 7.4–7.8 until day 64 and slightly drops to 6.6 when the inhibition occurs on day 77. During the first three stages of the feeding rates, LCFA concentration slightly increases with time from 42 mg/L (day 0) to 616 mg/L (day 48). At the last stage, LCFAs show a sharp increase from 620 mg/L to 2602 mg/L during days 70–79, which is consistent with the period when gas production is inhibited. In more detail, a significant drop in the gas production rate occurs on day 77, when the LCFA concentration is 1686 mg/L. Actually the increase in LCFAs slightly precedes the decrease in biogas production. There is no great difference in the composition of LCFAs except on day 79 as shown in Table 1. Palmitic acid always has the highest percentage in C8–C22 fatty acids, and accounts for 47.5 ± 15.7 wt % of the total C8–C22 fatty acids on average throughout the experiment. Oleic acid follows palmitic acid and accounts for 26.7 ± 12.4 wt %. During the sudden increase in LCFAs at days 73 and 77, the percentage of palmitic acid increases to 75 wt %. As Table 1 shows, the total LCFA concentration consists majorly of palmitic acid from the initial period to day 77; hence palmitic acid should be monitored as a priority in view of these above findings.

Table 1. The main composition of LCFAs in digestate samples ($n = 1$).

Day	Concentration (mg/L)					Total
	C16:0	C16:1	C18:0	C18:1	C18:2	
30	115	0	36	76	0	227
40	147	0	48	116	18	328
42	136	3	51	72	26	333
44	154	11	49	174	42	473
48	280	4	103	130	33	616
64	229	12	87	173	21	543
70	204	14	87	267	31	620
73	924	14	122	79	0	1229
77	1267	15	140	119	13	1686
79	918	85	235	788	352	2602

**Figure 4.** (a) Time courses of gas production rates and feeding rate of de-oiled grease trap waste (GTW); and (b) The change of pH and long-chain fatty acids (LCFA) concentration during the semi-continuous experiment.

3.2.2. Quartz Crystal Microbalance Measurements of Anaerobic Digestate Samples

Digestate samples were taken from the reactor during the semi-continuous operation at various intervals from day 30 to 79 (Table 1). To reduce LCFA concentration to below 100 mg/L, these samples were diluted 40 times with water. After the dilution and pH adjustment to 10.7, the samples were applied to the QCM sensor. Figure 5a indicates a comparison trend between LCFA concentration and absolute frequency-shift rate. All measurements were carried out in the same way as above, except the sample taken at day 79. The sample at day 79 shows very high increasing rates of resonance residence and reaches 1000 ohm at about 100 s; then the frequency change becomes unstable. As such, the frequency-shift rate of that sample is calculated using a shorter linear range (50–100 s). The frequency-shift rates maintain a low level below 0.7 Hz/s during days 30–48 and then increase to a slightly higher level around 1.0 Hz/s at days 64 and 70. A sharp elevation of the frequency-shift rate occurs with a notable increase in LCFA during days 73–79. As a result, there is a significant correlation ($R^2 = 0.9751$, p -value < 0.0001) between the frequency-shift rates and LCFA.

The results shown in Figure 5b indicate that LCFA concentrations in unknown samples can be determined using an external calibration curve. Figure 5b plots the values of frequency-shift rate versus those of LCFA concentration. As discussed above, there are clear linear relationships between

two types of values in both palmitate and digestion samples. Furthermore, the two lines are almost consistent with each other. This means that a regression line equation obtained from palmitate samples allows for an estimate of LCFA concentration in a digestate sample from the measured frequency-shift rate of the sample.

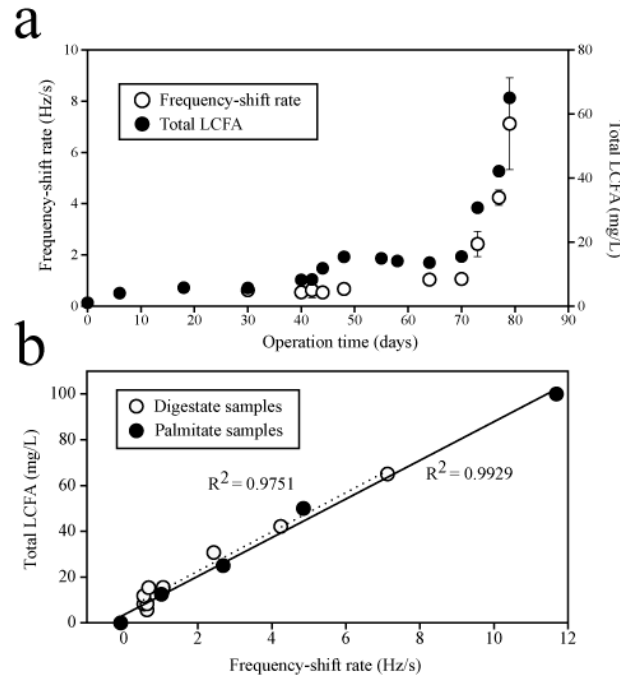


Figure 5. (a) Time courses of QCM frequency-shift rates ($n = 3$) and LCFA concentrations of anaerobic digestate samples; and (b) Comparison of relationships between frequency-shift rates and LCFA concentrations in digestate and palmitate samples. Total LCFA values in Figure 5 are the concentrations of diluted samples before measurements.

From the view point of practical use, real anaerobic digestate has many organic contaminants. Above all, triglyceride is the major contaminant in de-oiled GTW-AD, and has the possibility of affecting the water-solubility of LCFA. According to Schwarzenbach et al. [25], the solubility of an organic compound (i) between a liquid organic mixture (organic compound (i) and organic solvent) and an aqueous phase is defined as the following equation.

$$\gamma_w^{-1} = C_{tot}^{sat} \cdot \exp\left(\frac{\Delta S_m}{R} \left[\frac{T_m}{T} - 1\right]\right) = C_{tot}^{sat} \cdot \exp\left(\frac{\Delta H_{fus}}{RT_m} \left[\frac{T_m}{T} - 1\right]\right) \quad (3)$$

$$C_{i w} = \gamma_{i org} \cdot x_{i org} \cdot \gamma_w^{-1} = \gamma_{i org} \cdot x_{i org} \cdot C_{tot}^{sat} \cdot \exp\left(\frac{\Delta H_{fus}}{RT_m} \left[\frac{T_m}{T} - 1\right]\right) \quad (4)$$

where C_{tot}^{sat} is the total water-solubility of compound (i), ΔH_{fus} is enthalpy of fusion (J/mol), T_m is melting temperature (K), $\gamma_{i org}$ is the activity coefficient of compound (i) in the organic phase, and $x_{i org}$ is the mole fraction in the organic solvent (mol/mol-solvent). When $x_{i org}$ is lower than 1, the mixture of palmitic acid and triolein can be considered as organic liquid. On the basis of the experimental study on equilibria in fatty acid/triglyceride systems, the mixture of palmitic acid and triolein can be considered an ideal solution [32]; thus, $\gamma_{i org}$ is 1. From our recent studies [33], ΔH_{fus} and T_m of palmitic acid are 335.6 K and 55,840 J/mol, respectively. Therefore, the water-solubility of palmitic acid in the mixture of palmitic acid, triolein, and water is expressed as follows:

$$C_{pal w} = 12.5 x_{pal tri} \cdot C_{tot}^{sat} \quad (5)$$

This result suggests that even if $x_{pal\ tri}$ is only 0.08, palmitic acid can maintain the same level of solubility when applied as a sole contaminant. Realistically it is found that the effect of organic contaminants on the solubility of LCFA can be ignored. These results confirm that the newly developed QCM sensor can detect the increasing trend in LCFAs prior to the inhibition of biogas production.

3.3. Validation of the New Method

Reproducibility of the coated QCM sensor was evaluated by the repeated measurements of anaerobic digestate sample (day 42) using the single QCM disc; the obtained results are presented in Figure 6. According to the researchers, RSD should not exceed 20% [34]. In this case, as shown in Figure 6, there is a slight variation among the values of frequency-shift rates and the RSD is 13.6%, which is within the proper range. However this RSD value is higher than those obtained using GC by Neves et al. [34]. In terms of accuracy, GC analysis seems to perform better. The variation of frequency-shift rates is likely due to the manual-based coating method in this study because the QCM disc is newly coated every time. Actual, the manually coated thin film does not look uniform; thus a coating equipment should be used to improve reproducibility.

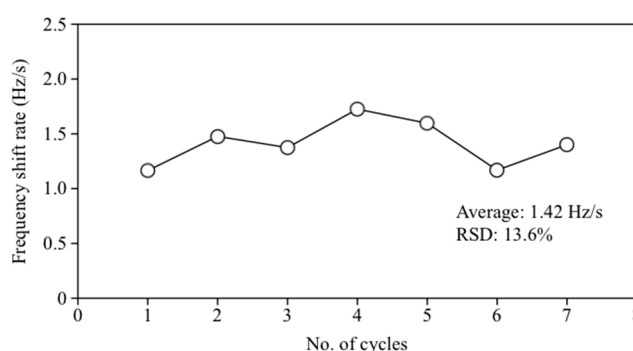


Figure 6. Reproducibility of frequency-shift rates from the same QCM sensor ($n = 7$).

It has been shown by Pereira et al. [35] that the inhibition is more closely related to the LCFAs adsorbed onto microbial cells (so called biomass-associated LCFAs) than the free LCFAs in liquid phase. Therefore it is more useful for AD to measure biomass-associated LCFAs with the QCM sensor. However, it is still unclear if the present pretreatment method including pH adjustment and heating can elute the biomass-associated LCFAs into alkaline water. An additional series of experiments was carried out to understand the distribution ratio of LCFAs between water and solid (biomass). Table 2 summarizes LCFA recoveries in the pretreatment using three different digestate samples. The results indicate that the pretreatment method used in this study cannot recover biomass-associated LCFAs; namely the QCM sensor might measure free LCFAs in liquid phase. The LCFAs in the sediment accounts for 36%–58% of the total LCFAs in the sludge and the mass concentrations in 1 g TSS are 23 mg/g-TSS (Sludge A), 25 mg/g-TSS (Sludge B) and 49 mg/g-TSS (Sludge C), respectively. Sludge C, which was strongly inhibited by LCFAs, accumulates more LCFAs in biomass. Even so, it seems that similar increasing trends can be obtained between total LCFA concentrations and frequency-shift rates since LCFAs in supernatant is increased with total LCFA concentrations in sludge as shown in Table 2. To improve recovery of biomass-associated LCFAs, the modified pretreatment method should be designed. Neves et al. [34] successfully extracted LCFAs in organic phase from solid samples. Since dissociation elutes LCFAs in organic solvent into water, it might be better that the pH adjustment follows the first extraction using organic solvent.

Table 2. LCFA recoveries in the supernatant and sediment obtained after pretreatment for QCM sensor ($n = 3$).

Sample	TSS	Total LCFA in Supernatant	Total LCFA in Sediment	Recovery ¹
	g/L	mg/L-sludge _{fed}	mg/L-sludge _{fed}	%
Sludge A	10.4	205 ± 74	244 ± 22	46%
Sludge B	14.6	227 ± 29	396 ± 65	36%
Sludge C	19.1	1116 ± 562	629 ± 27	64%

¹ Percentage of LCFAs extracted in alkaline supernatant.

From the above discussion, it was found that the proposed method is less accurate in terms of reproducibility than GC analysis. The conventional GC analysis should be used to know more scientifically reliable and detailed LCFA data. Nevertheless the proposed method offers the advantage of providing results by a simple device in a shorter time as the overall experiment, including the pretreatment for each sample, takes only 1 h. A QCM sensor is considered a cost-effective device [36], whereas consumable costs depend on a costly quartz disc. The above-mentioned result indicates that the simple coating method enables the regeneration of sensor response, which contributes to reducing the cost. Previously, it has been reported that a QCM sensor with a silver electrode is easily reacted with hydrogen sulfide gas that microorganisms produce [37]. In this case, each measurement requires only a few minutes to detect LCFA with the QCM sensor. Therefore, the sensor can be operated in a batch mode to reduce exposure of the sensor to such a corrosive compound. From these reasons, it is believed that the QCM sensor is feasible for practical analysis of LCFAs in anaerobic digestate.

4. Conclusions

A polymer-coated selective QCM sensor was developed for the quantitative detection of LCFA produce from anaerobic degradation of oily organic wastes. The dissociation of fatty acids at an alkaline pH greatly improved sensor response and, moreover, allowed selective detection of palmitate under presence of triglyceride. The sensor showed a good linear relationship between palmitate concentrations and QCM frequency shift within the practical LCFA concentration range (0–100 mg/L). The QCM measurements using real anaerobic digestate revealed that there is a significant correlation ($R^2 = 0.9751$ and p -value < 0.0001) between the frequency-shift rates and LCFA. It can be concluded that our QCM sensor is a useful tool to monitor the increasing trends in LCFA prior to the inhibition of biogas production and, thereby, that makes it easy to timely reduce the inhibition by adding calcium or decreasing organic loading rate.

Acknowledgments: We thank Young-Han Kim of the Department of Chemical Engineering, Dong-A University (yhkim@dau.ac.kr), for his valuable suggestions and help. This work was supported by KAKENHI of the Japan Society for Promotion of Science (JSPS) (15K18148).

Author Contributions: Takuro Kobayashi and Hidetoshi Kuramochi performed the experiments and analysis; Kouji Maeda contributed the materials and tools; Kaiqin Xu contributed to editing the paper.

Conflicts of Interest: The authors declare no conflict of interest.

References

1. Kobayashi, T.; Kuramochi, H.; Xu, K.Q. Variable oil properties and biomethane production of grease trap waste derived from different resources. *Int. Biodeterior. Biodegrad.* **2016**. [[CrossRef](#)]
2. Yalcinkaya, S.; Malina, J.F. Model development and evaluation of methane potential from anaerobic co-digestion of municipal wastewater sludge and un-dewatered grease trap waste. *Waste Manag.* **2015**, *40*, 53–62. [[CrossRef](#)] [[PubMed](#)]
3. Shin, H.; Kim, S.H.; Lee, C.Y.; Nam, S.Y. Inhibitory effects of long-chain fatty acids on VFA degradation and beta-oxidation. *Water Sci. Technol.* **2003**, *47*, 139–146. [[PubMed](#)]

4. Alves, M.M.; Mota, V.J.A.; Álvares, P.R.M.; Pereira, M.A.; Mota, M. Effects of lipids and oleic acid on biomass development in anaerobic fixed-bed reactors. Part II: Oleic acid toxicity and biodegradability. *Water Res.* **2001**, *35*, 264–270. [[CrossRef](#)]
5. Cho, H.S.; Moon, H.S.; Lim, J.Y.; Kim, J.Y. Effect of long chain fatty acids removal as a pretreatment on the anaerobic digestion of food waste. *J. Mater. Cycles Waste Manag.* **2013**, *15*, 82–89. [[CrossRef](#)]
6. Pereira, M.A.; Pires, O.C.; Mota, M.; Alves, M.M. Anaerobic biodegradation of oleic and palmitic acids: Evidence of mass transfer limitation caused by long chain fatty acid accumulation onto anaerobic sludge. *Biotechnol. Bioeng.* **2005**, *92*, 15–23. [[CrossRef](#)] [[PubMed](#)]
7. Kobayashi, T.; Kuramochi, H.; Maeda, K.; Tsuji, T.; Xu, K.Q. Dual-fuel production from restaurant grease trap waste: Bio-fuel oil extraction and anaerobic methane production from the post-extracted residue. *Bioresour. Technol.* **2014**, *169*, 134–142. [[CrossRef](#)] [[PubMed](#)]
8. Palatsi, J.; Laurenzi, M.; Andrés, M.V.; Flotats, X.; Nielsen, H.B.; Angelidaki, I. Strategies for recovering inhibition caused by long chain fatty acids on anaerobic thermophilic biogas reactors. *Bioresour. Technol.* **2009**, *100*, 4588–4596. [[CrossRef](#)] [[PubMed](#)]
9. Roy, F.; Albagnac, G.; Samain, E. Influence of calcium addition on growth of highly purified syntrophic cultures degrading long-chain fatty acids. *Appl. Environ. Microbiol.* **1985**, *49*, 702–705. [[PubMed](#)]
10. Koster, I.W. Abatement of long-chain fatty acid inhibition of methanogenesis by calcium addition. *Biolog. Wastes* **1987**, *22*, 295–301. [[CrossRef](#)]
11. Wu, L.; Kobayashi, T.; Kuramochi, H.; Li, Y.Y.; Xu, K.Q. Recovery strategies of inhibition for mesophilic anaerobic sludge treating the de-oiled grease trap waste. *Int. Biodeterior. Biodegrad.* **2015**, *104*, 315–323. [[CrossRef](#)]
12. Lalman, J.A.; Bagley, D.M. Anaerobic degradation and methanogenic inhibitory effects of oleic and stearic acids. *Water Res.* **2001**, *35*, 2975–2983. [[CrossRef](#)]
13. Neves, L.; Oliveira, R.; Alves, M.M. Fate of LCFA in the co-digestion of cow manure, food waste and discontinuous addition of oil. *Water Res.* **2009**, *43*, 5142–5150. [[CrossRef](#)] [[PubMed](#)]
14. Pitk, P.; Palatsi, J.; Kaparaju, P.; Fernández, B.; Vilu, R. Mesophilic co-digestion of dairy manure and lipid rich solid slaughterhouse wastes: Process efficiency, limitations and floating granules formation. *Bioresour. Technol.* **2014**, *166*, 168–177. [[CrossRef](#)] [[PubMed](#)]
15. Si, P.; Mortensen, J.; Komolov, A.; Denborg, J.; Møller, P.J. Polymer coated quartz crystal microbalance sensors for detection of volatile organic compounds in gas mixtures. *Anal. Chim. Acta* **2007**, *597*, 223–230. [[CrossRef](#)] [[PubMed](#)]
16. Lu, H.H.; Rao, Y.K.; Wu, T.Z.; Tzeng, Y.M. Direct characterization and quantification of volatile organic compounds by piezoelectric module chips sensor. *Sens. Actuators B* **2009**, *137*, 741–746. [[CrossRef](#)]
17. Escuderos, M.E.; Sanchez, S.; Jimenez, A. Quartz crystal microbalance (QCM) sensor arrays selection for olive oil sensory evaluation. *Food Chem.* **2011**, *124*, 857–862. [[CrossRef](#)]
18. Escuderos, M.E.; Sánchez, S.; Jiménez, A. Virgin olive oil sensory evaluation by an artificial olfactory system, based on quartz crystal microbalance (QCM) sensors. *Sens. Actuators B* **2010**, *147*, 159–164. [[CrossRef](#)]
19. Yang, Z.P.; Zhang, C.J. Designing of MIP-based QCM sensor for the determination of Cu(II) ions in solution. *Sens. Actuators B* **2009**, *142*, 210–215. [[CrossRef](#)]
20. Gupta, V.K.; Yola, M.L.; Eren, T.; Atar, N. Selective QCM sensor based on atrazine imprinted polymer: Its application to wastewater sample. *Sens. Actuators B* **2015**, *218*, 215–221. [[CrossRef](#)]
21. Maeda, K.; Hayashi, A.; Iimura, K.; Suzuki, M.; Hirota, M.; Asakuma, Y.; Fukui, K. Generation of nanometer-scale crystals of hydrophobic compound from aqueous solution. *Chem. Eng. Process.* **2005**, *44*, 941–947. [[CrossRef](#)]
22. Ichihara, K.; Fukubayashi, Y. Preparation of fatty acid methyl esters for gas-liquid chromatography. *J. Lipid Res.* **2010**, *51*, 635–640. [[CrossRef](#)] [[PubMed](#)]
23. Kanicky, J.R.; Poniatowski, A.F.; Mehta, N.R.; Shah, D.O. Cooperativity among molecules at interfaces in relation to various technological processes: Effect of chain length on the pKa of fatty acid salt solutions. *Langmuir* **2000**, *16*, 172–177. [[CrossRef](#)]
24. Kanicky, J.R.; Shah, D.O. Effect of degree, type, and position of unsaturation on the pKa of long-chain fatty acids. *J. Colloid Interface Sci.* **2002**, *256*, 201–207. [[CrossRef](#)] [[PubMed](#)]
25. Schwarzenbach, R.P.; Gschwend, P.M.; Imboden, D.M. *Environmental Organic Chemistry*, 2nd ed.; Wiley-Interscience: Hoboken, NJ, USA, 2003; p. 1313.

26. Yalkowsky, S.H.; He, Y.; Jain, P. *Handbook of Aqueous Solubility Data*, 2nd ed.; CRC Press: Boca Raton, FL, USA, 2010; p. 1620.
27. Ying, Z.; Jiang, Y.; Du, X.; Xie, G.; Yu, J.; Wang, H. PVDF coated quartz crystal microbalance sensor for DMMP vapor detection. *Sens. Actuators B* **2007**, *125*, 167–172. [[CrossRef](#)]
28. Ayad, M.M.; Torad, N.L. Alcohol vapours sensor based on thin polyaniline salt film and quartz crystal microbalance. *Talanta* **2009**, *78*, 1280–1285. [[CrossRef](#)] [[PubMed](#)]
29. Reipa, V.; Purdum, G.; Choi, J. Measurement of nanoparticle concentration using quartz crystal microgravimetry. *J. Phys. Chem. B* **2010**, *114*, 16112–16117. [[CrossRef](#)] [[PubMed](#)]
30. Buck, R.P.; Lindner, E.; Kutner, W.; Inzelt, G. Piezoelectric chemical sensors. *Pure Appl. Chem.* **2004**, *76*, 1139–1160. [[CrossRef](#)]
31. Wu, L.; Kobayashi, T.; Kuramochi, H.; Li, Y.Y.; Xu, K.Q. Improved biogas production from food waste by co-digestion with de-oiled grease trap waste. *Bioresour. Technol.* **2016**, *201*, 237–244. [[CrossRef](#)] [[PubMed](#)]
32. Nishimura, K.; Maeda, K.; Kuramochi, H.; Nakagawa, K.; Asakuma, Y.; Fukui, K.; Osako, M.; Sakai, S. Solid-Liquid Equilibria in Fatty Acid/Triglycerol Systems. *J. Chem. Eng. Data* **2011**, *56*, 1613–1616. [[CrossRef](#)]
33. Yui, K.; Itsukaichi, Y.; Kobayashi, T.; Tsuji, T.; Fukui, K.; Maeda, K.; Kuramochi, H. Solid-liquid equilibria in the binary systems of saturated fatty acids or triglycerides (C12 to C18) + hexadecane. *J. Chem. Eng. Data* **2016**. [[CrossRef](#)]
34. Neves, L.; Pereira, M.A.; Mota, M.; Alves, M.M. Detection and quantification of long chain fatty acids in liquid and solid samples and its relevance to understand anaerobic digestion of lipids. *Bioresour. Technol.* **2009**, *100*, 91–96. [[CrossRef](#)] [[PubMed](#)]
35. Pereira, M.A.; Sousa, D.Z.; Mota, M.; Alves, M.M. Mineralization of LCFA associated with anaerobic Sludge: Kinetics, enhancement of methanogenic activity, and effect of VFA. *Biotechnol. Bioeng.* **2004**, *88*, 502–511. [[CrossRef](#)] [[PubMed](#)]
36. Pan, M.; Fang, G.; Lu, Y.; Kong, L.; Yang, Y.; Wang, S. Molecularly imprinted biomimetic QCM sensor involving a poly(amidoamine) dendrimer as a functional monomer for the highly selective and sensitive determination of methimazole. *Sens. Actuators B* **2015**, *207*, 588–595. [[CrossRef](#)]
37. He, F.; Cui, X.; Ren, J. A Novel QCM-based biosensor for detection of microorganisms producing hydrogen sulfide. *Anal. Lett.* **2008**, *41*, 2697–2709. [[CrossRef](#)]



© 2016 by the authors; licensee MDPI, Basel, Switzerland. This article is an open access article distributed under the terms and conditions of the Creative Commons Attribution (CC-BY) license (<http://creativecommons.org/licenses/by/4.0/>).